Article ID: 1001-3555(2018)06-0546-09

Mediating the Catalytic Selectivity of Au Nanoclusters by Ligand Engineering

GAO Gui-qi[2], CHONG Han-bao[1,2], LI Guang[1*]

(1. *School of Physics and Material Science, Anhui University, Hefei* 230601, *China*;
2. *Institute of Physical Science and Information Technology, Anhui University, Hefei*, 230601, *China*)

Abstract: It was well-established that the thiolate ligands laid significant influence on the catalytic properties of protected Au nanoclusters (NCs for short), especially the selectivity. In this work, catalytic nitro reduction is investigated over nanocluster catalyst. The electron-withdrawing property of thiolates renders the surface positively charged, which results in less aniline derivatives. The conversion is found to augment a lot after complete removal of capping thiolates, owing to the accessibility of active sites on Au NCs. Furthermore, a range of functionalized substrates are investigated for the universality of this catalytic reaction, and the composite catalysts show good tolerance to functional groups. Moreover, the exterior ligands were gradually peeled off by thermal treatment through controlling the temperature under vacuum, and the as-prepared catalysts were characterized by TEM, FTIR measurements. Using these catalysts, the relationship between the extent of ligand removal and the catalytic activity/selectivity was investigated.

Key words: ligand effect; selectivity; Au nanoclusters; nanocatalysis

CLC number: O643.36 **Document code**: A

Recently, gold nanoclusters (NCs for short) have gained popularity for their catalytic properties owing to the quantum effect and high volume/surface ratio[1]. Among them, NCs with ultra-small size (less than 2 nm with metallic kernel) glint the most because of high surface-to-volume ratio, the surface geometric effect the electronic effect, as well as the quantum size effect[2-3]. Additionally, the atomically precise NCs pose the potential for fully understanding the structure-property correlations owing to their exact structure[4-6]. By investigating the size effect on catalytic activity, it has been proved that clusters with size at about 2 nm exhibit the best performance[7-9]. Besides the size dependence, previous literature paid tremendous attention to the expansion of reaction type[10-14], better activity[15-16], synergistic effect[17-20], and mechanism research[21-23].

The ligands bonded on the surface of gold NCs block the contact between substrate and gold, which results in low conversion in catalysis; however, organic ligands could also modulate the electronic states of NCs[24-26]. Additionally, the electronic states have a major influence on the catalytic conversion, but also the product selectivity[27-33]. Li *et al.* unravelled that the species of capping agents could tune the electronic and catalytic properties of Au NCs theoretically and experimentally[34]. Xie *et al.* elucidated the catalytic performance of NCs could be interfered by the length of S ligands and functional moiety[35]. Obviously, the capping ligand is a significant parameter affecting the catalyst activity, and the management of ligand could hopefully be an efficient way to design better catalyst with enhanced performance. The thiols are the most popular ligands in the synthesis of Au NCs[36-39] since the Au-S bond is much stronger than any others, correspondingly, they affect the performance of Au NCs catalyst quite dramatically.

In this paper $Au_{25}L_{18}$ ($L = PhC_2H_4S$) was employed as a model catalyst to evaluate the influence of capping agent on the catalytic activity and selectivity. The reduction of nitrobenzene usually gives rise to phe-

Received date: 2018-09-27; **Revised date**: 2018-10-10.

Foundation: Supported by Doctoral Startup Foundation of Anhui University (grant no. 10113190077), the Anhui Provincial Natural Science Foundation (grant no. 1608085QB39), and the National Natural Science Foundation of China (grant no. 51402001).

First author: GAO gui-qi, female, born in 1987 doctor.

Corresponding author: E-mail: gaogq@ahu.edu.cn, Tel:0551-63861856.

nylhydroxylamine, aniline, azobenzene, azoxybenzene and hydrazobenzene as products. Hence, it is introduced as a probe reaction. The capping ligands were gradually removed by increasing the incineration temperature step by step. As the NCs readily aggregate under high temperatures, the heterogeneous support thus becomes indispensable for preventing aggregation. Porous structured nickel silicates are used as the support; their high surface area of 280 m^2/g efficiently inhibits aggregation of NCs, and the chemically inert character rules out their interference to the investigation of ligand effect.

The nickel silicates and Au_{25} NCs were synthesized according to the previous literature[40-41]. The immobilization of Au NCs was accomplished by means of adsorption and calcination. After collecting the deposit of centrifuged solution, the Au_{25}/Ni-SiO_2 composite was dried under vacuum at 50 ℃. By increasing the incineration temperature, which was 150, 200, 250 and 300 ℃ step by step, partial to complete S ligand removal was achieved. Heating for 2 h at 300 ℃ was enough to completely peel off the capping agents based on the TGA analysis[26], avoiding severe aggregation of NCs. All the ligands were untouched if the composite hadn't been subject to the heat treatment. The unprocessed composite catalysts were introduced as the basis for comparison. Hereafter, the composite catalysts treated at different temperatures were referred as Au_{25}@ Ni-SiO_2(RT, referring to room temperature, which was not processed by heating), Au_{25} @ Ni-SiO_2(150), Au_{25}@ Ni-SiO_2(200), Au_{25}@ Ni-SiO_2(250) and Au_{25}@ Ni-SiO_2(300), respectively.

1 Experiments and characterization

All the chemicals and reagents are purchased from Aladdin Corporation with GR grade. TLC plates (Merck Silica Gel 60 F254) were used for analytical TLC, and Merck Kieselgel 200~300 was used for preparative column chromatography. Conversion and selectivity were measured with Shimadzu (Japan) GC 2010 plus. TEM images were obtained by JEM 2100 (Japan). The intermediates and product identification was carried out by Saturn2200 GC-MS of Varian (America). The samples were weighed with a Mettler Toledo MX5 scale with d=0.1 ug (Swiss). IR spectra were recorded with Bruker Hyperion Vertex80 (German) by using KBr carrier. The quantification of Au content of the composite catalysts was assessed by ICP AES (Inductively Coupled Plasma Atomic Emission Spectrometer) of I-RIS intrepid II XSP which is purchased from Thermo Electron (America). The specific surface area of samples was obtained based on an N_2 adsorption-desorption isothermal analysis (V-Sorb 2800P, Gold APP Instruments, China) with the Brunauer-Emmett-Teller (BET) model.

The synthesis of $Au_{25}(SCH_2CH_2Ph)_{18}$-$TOA^+$ (TOA = tetraoctylammonium bromide) and porous nickel silicates were described in previous literature. After both were prepared, 5 mg Au_{25} (dissolved in a spot of THF, short for tetramethylene oxide) was added into 100 mL ethanol along with 650 mg silicates. The mixture was sonicated for 10 minutes, followed by stirring for 2 h. Afterwards, the mixture was centrifuged to remove unabsorbed NCs, and the sediment was dried under vacuum at 50 ℃. The different catalysts were treated at 150, 200, 250 and 300 ℃ for 2 h. The calcination program was set as room temperature heating up to 50 ℃ for 30 min, preserving for another 30 min before taking 2 h heating up to 150 ℃, and finally preserving for 2 h before cooling down. A round bottomed flask was charged with 0.2 mL (2 mmol) nitrobenzene and 0.112 g $NaBH_4$ (4 mmol), 30 mg immobilized catalyst (Au 6.1×10^{-3} mmol), and 2 mL EtOH/2 mL H_2O. After stirring at 90 ℃ under vacuum for 2 hours, the reaction was completed. The product was analyzed by GC-MS.

2 Results and discussion

The immobilization of Au NCs was accomplished by blending the support and NCs in ethanol, then drying the sediments after collecting them. All the supported catalysts were prepared in the same batch to unify the Au loading, but treated at different temperatures to control the different degree of ligand desorption. The Au loading was determined by ICP-AES tests to be 0.4% wt. The BET surface of as-prepared Ni-

SiO_2 sphere is 280 $m^2 \cdot g^{-1}$, which is higher than amorphous material.

The unheated Au_{25}@ Ni-SiO_2 composite and other catalysts calcined at 150, 200, 250 and 300 ℃ were all characterized by HRTEM to determine the size distribution after immobilization and heat treatment (Fig.1).

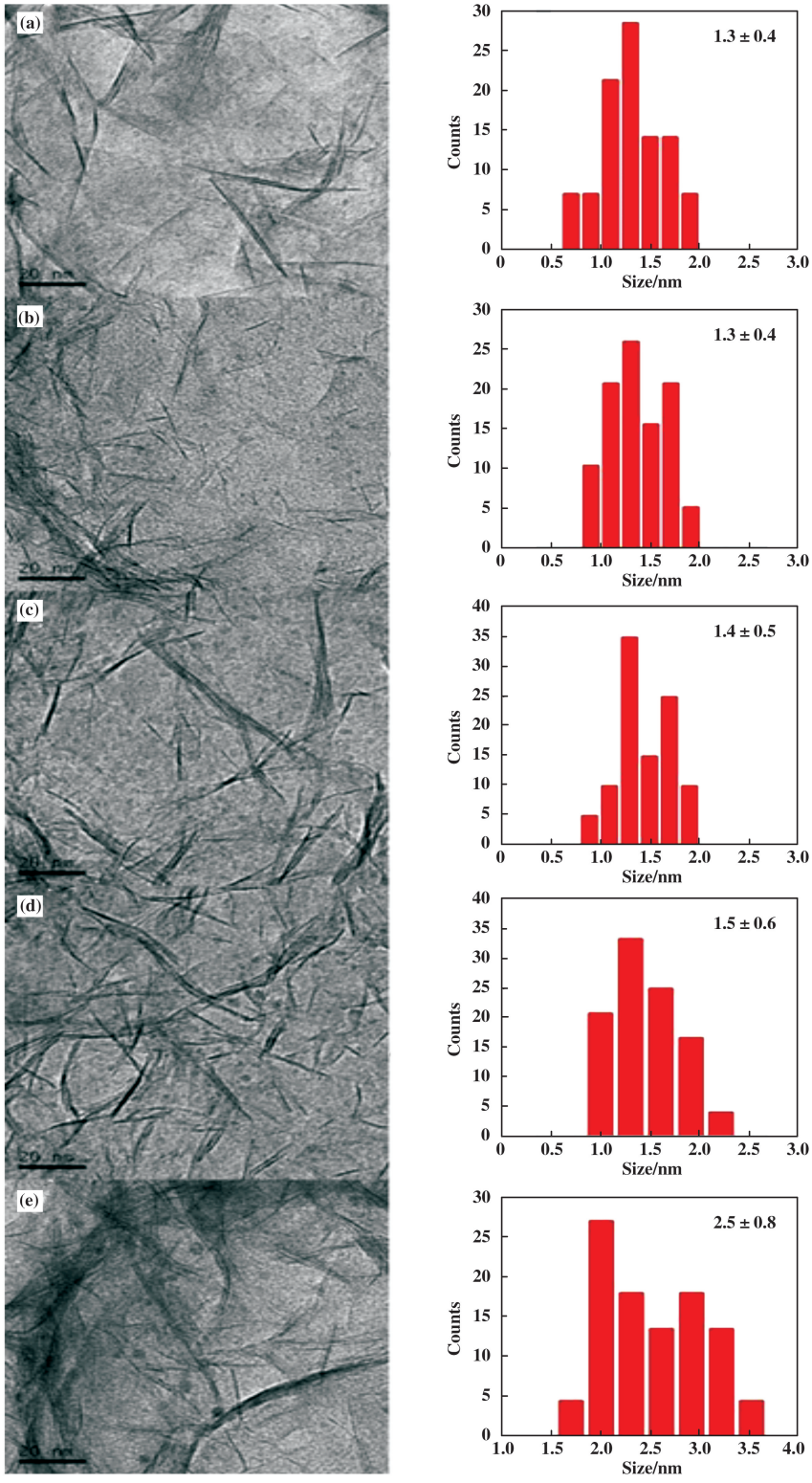

Fig.1 TEM images and size histograms of NCs supported on porous Ni-SiO_2 spheres, the scale bar is 20 nm in each panel The calcination temperature is none (a), 150 ℃ (b), 200 ℃ (c), 250 ℃ (d), 300 ℃ (e), respectively

The average size of Au_{25}@ Ni-SiO_2 (RT) is 1.3 nm, indicating that the immobilization procedure didn't lead to the aggregation of Au_{25} (Fig. 1a).

TGA analysis showed no ligand loss under 170 ℃, thus the structure of Au_{25} should not collapse given that the $Au_{25}(SR)_{18}$ structure is the most thermodynamically stable one. The 150 ℃-treated Au_{25}@ Ni-SiO_2 did not show any observable size enhancement (Fig. 1b). However, the composite heated at higher temperature led to slight aggregation: the average sizes were larger, and the size distribution was broadened: 1.4±0.5 nm for 200 ℃ and 1.5±0.6 nm for 250 ℃; when the heating temperature was increased to 300 ℃, the size increased further (2.5±0.8 nm) larger than the starting one (1.3 nm±0.4 nm). The high temperature was required to stripe off the capping ligands from the surface of Au NCs; slight aggregation was the cost. Fortunately, the size alteration was negligible, thus it is still reliable to conclude the relationship between catalytic property and ligand effect.

FTIR was employed to detect the residue ofthiolate ligand (Fig. 2). Since the Au loading was as low as

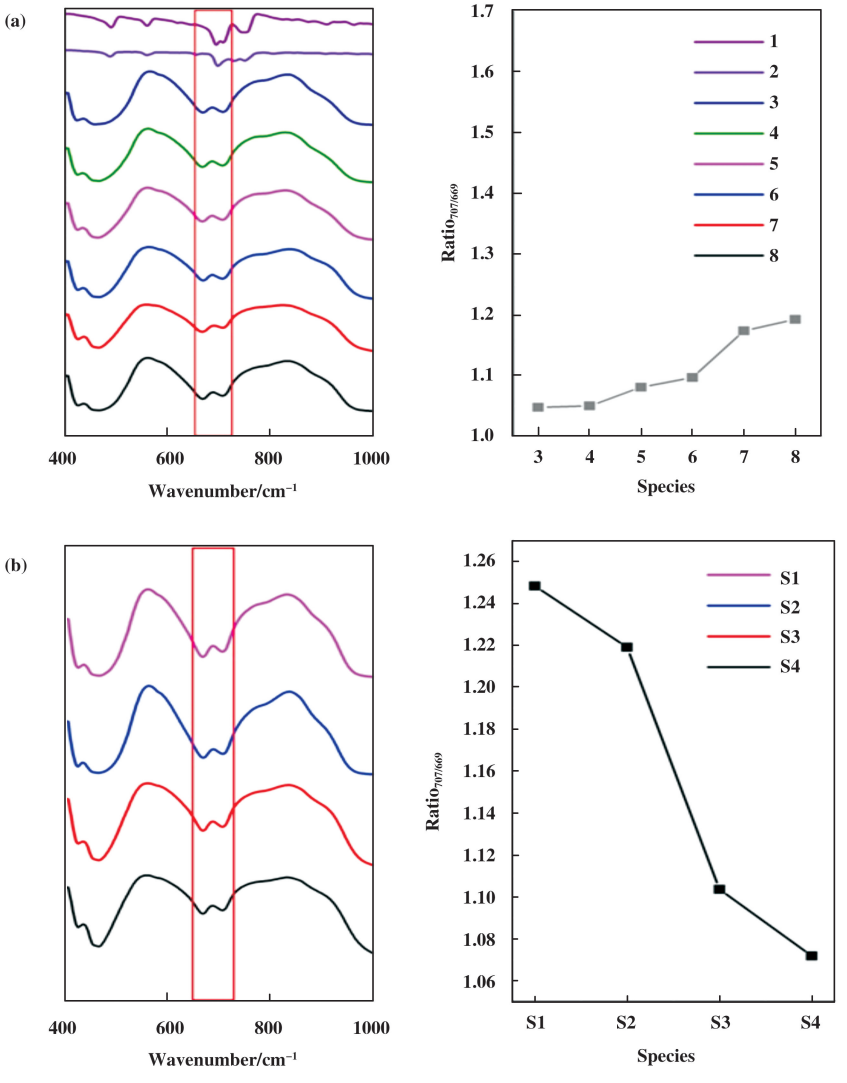

Fig.2 (a) FTIR spectra of Au_{25}, Ni-SiO_2 and supported catalysts calcined at different temperature (left) and ratio of transmission between 707 cm^{-1} and 669 cm^{-1} (right); 1-8 stand for $PhCH_2CH_2SH$, Au_{25}, Au_{25}@ Ni-SiO_2 (RT), Au_{25}@ Ni-SiO_2 (150), Au_{25}@ Ni-SiO_2 (200), Au_{25}@ Ni-SiO_2 (250), Au_{25}@ Ni-SiO_2 (300), Ni-SiO_2, respectively. (b) FTIR spectra of pure Ni-SiO_2 calcined at different temperature (S1-150 ℃, S2-200 ℃, S3-250 ℃, S4-300 ℃) and ratio of transmission between 707 and 669 cm^{-1}

0.4% wt, and the ligand content in the NCs was only 37%, IR was a better method to distinguish the organic remaining than using other conventional instruments. The typical IR adsorption peak of mono-substituted benzene ring is at 694 cm^{-1}, while it shifts to 700 cm^{-1} when the PhC_2H_4S was bonded to the Au NCs, and further shifts to 707 cm^{-1} when the NCs are immobilized on the Ni-SiO_2 spheres. The adsorption band centered at 669 cm^{-1} is assigned to the intrinsic sphere support. However, another adsorption band centered at 707 cm^{-1} was overlapped with the organic component, as a result, the two peaks merged into a bigger one. It is thus not possible to quantify the exact amount of S residue of all the catalysts, considering the film thickness of IR samples being difficult to consolidate. Fortunately, the ratio between 707 and 669 cm^{-1} could be utilized as an efficient tool to represent the concentration of S remaining in the composite catalysts, because the transmission at 669 cm^{-1} is always linear with the sample content. As shown in Fig.2a, the 707 cm^{-1} peak continually became weaker along with the increasing calcination temperature (left). The plot on the right panel gave more intuitive result: no ligand loss between 150 ℃ and room temperature; and then gradual loss was observed when the temperature was further augmented. The structure should collapse in the 300 ℃ treatment for 2 h, which was verified by TGA and TEM images, and the organic capping agents were totally stripped off from the Au surface. Since the Ni-SiO_2 supports were also incinerated under the same circumstance, the factor had to be taken into account (see Fig.2b). However, it was observed the transmission ratio between 707 and 669 cm^{-1} decreased in responding to gradually increased heating temperature, which was quite opposite to the Au@ Ni-SiO_2 case. The outcome further suggests the gradual loss of capping ligands.

Hydrogenation of nitrobenzene was investigated as a model reaction to evaluate the ligand effect on the catalytic properties. The products generally include aniline (referred to AN), azobenzene (AZO) and azoxybenzene (AXY). Control experiments were performed to confirm the catalytically active component. The extreme condition of 90 ℃ (with no catalyst) gave rise to a little conversion and the product was completely AXY (Fig.3, item 0), and pure Au_{25} gave a little higher

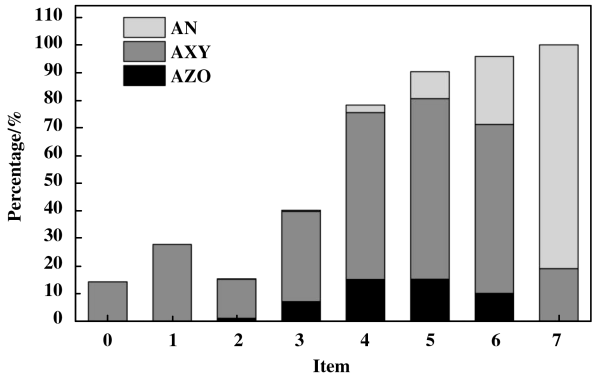

Fig.3 Conversion and selectivity of nitrobenzene catalyzed by all kinds of catalysts. 0 ~ 7 stand respectively for blank, Au_{25}, Ni-SiO_2, Au_{25} @ Ni-SiO_2 (RT), Au_{25} @ Ni-SiO_2 (150), Au_{25} @ Ni-SiO_2 (200), Au_{25} @ Ni-SiO_2 (250), Au_{25}@ Ni-SiO_2 (300). The height of the whole bar is the conversion percentage, the ratio between individual bars of different color is the selectivity

than that (item 1). Ultra-small NCs were readily aggregated under these circumstances, which resulted in poor activity. The item 2 ruled out the support as the active component, thus it acts as an essentially inert support in our system. The Ni-SiO_2 support was supposed to protect the NCs from detaching and aggregating. However, without the annealing process, the physically adsorbed NCs could not avoid the activity drop (item 3). Simultaneously, more AZO was generated and AN emerged. After annealing at 150 ℃, the supported catalysts gave rise to a conversion jump while more AN and AZO were observed. Along with the increasing sintering temperature, the conversion exhibited a linear enhancement, and the selectivity preference exhibited an upside down shift: AZO decreased to none and the primary product turned into AN.

After high temperature calcination, the Au_{25} NCs were not themselves anymore. Given that the NC size didn't display severe aggregation, it was still reasonable to conclude the relationship between catalytic performance and ligands concentration. The external organic agents more or less block active sites and thus lead to low catalytic activity. Correspondingly, the re-

moval of capping ligands releases some power on catalysis. More importantly, the ligand influence on the product selectivity became dazzling. There are two possible effects of the residual thiolates on the catalysis: steric and electronic effects[17]. Nevertheless, the steric hindrance of aniline was weak, while it was the primary product when all the capping agents were removed, suggesting that the steric effect was not the cause of the observed results. Au_{25} NCs with residual thiolates are more positively charged than the naked Au_{25} (i.e. essentially zero valence) owing to electron withdrawing by the S atoms, that's why the more reduced product aniline dominates in the products. Interestingly, the preference of AZO generated a down-para-curve pattern; it might be because of the more open catalyst surface and the more positively charged property.

The as-prepared catalysts were tested for functional group tolerance (Table 1). Only the two opposite catalysts, Au_{25}@Ni-SiO_2 (150) and Au_{25}@Ni-SiO_2 (300), were compared, as they gave the sharpest contrast. It was observed that derivatives with electron-withdrawing groups (entries 1, 4) were more active than those with electron-donating groups (entries 2 and 3), since the room temperature was enough to convert the substrates over the catalysts. The results were consistent with previous patterns though some byproducts were generated. The Au_{25}@Ni-SiO_2 (150) composite with S component gave rise to AXY derivatives as dominant products, while the other competitor yielded

Table 1 Hydrogenation of nitrobenzene derivatives catalyzed by Au_{25}@Ni-SiO_2 (150) and Au_{25}@Ni-SiO_2 (300) [a]

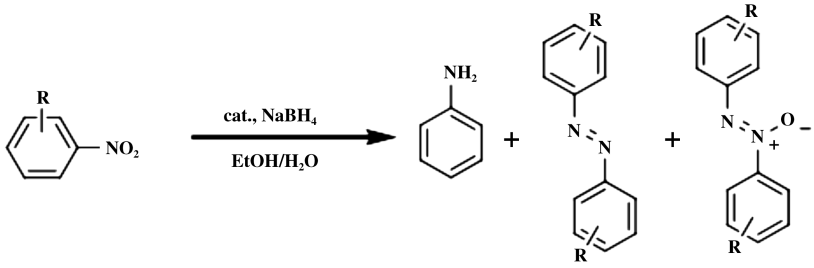

Entry	Substrate	Calcination Temperature /℃	Reaction Temperature /℃	Time /h	Conversion /%	Selectivity/%		
						Aniline	Azo	Axy
1	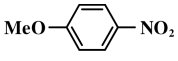	150	RT	8	21.2	15.4	19.2	65.4
		300			100	75.9	0	0
2	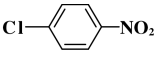	150	100	2	98.1	0	81.9	18.1
		300			100	65.7	11.9	22.4
3	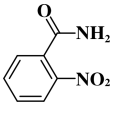	150	100	2	1.5	0	58.6	41.4
		300			100	50.8	24.9	24.3
4	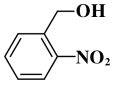	150	RT	8	0.6	69.3	30.7	0
		300			98.7	98.8	1.2	0

a. Reaction condition: 2 mmol substrate, 4 mmol $NaBH_4$, 30 mg immobilized catalyst (Au 6.1 * 10^{-3}mmol), and 2 mL ethanol/2 mL H_2O

overwhelmed anilines. The steric effect from substrates was considerable as well. The groups on the para-positions didn't interfere the contact between substrates and catalysts, and gave excellent conversion (entries 2). On the contrary, the groups on the ortho-position hindered the access to metal (entries 3 and 4), along with the exterior ligands of Au_{25}@ Ni-SiO_2(150) blocking the substrate approaching the active sites, hence low conversion at ambient conditions. As a result, the conversion was too low to make big differences on the product preference. These systematic results comprehensively verified the ligand effect on the catalytic properties, including activity and selectivity as scheme 1 illustrated.

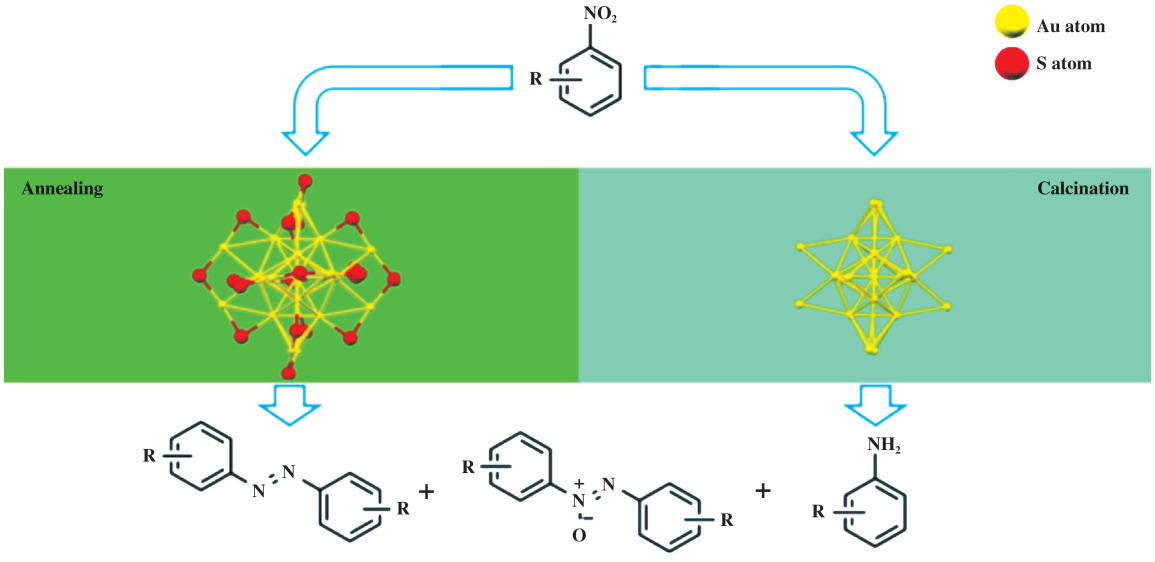

Scheme 1 Illustration of selective benzylamine reduction by protected and naked gold NCs

3 Conclutions

This work reveals that the exterior ligands of Au NCs have a great influence on the catalytic properties, in particular on the product selectivity. The electron-withdrawing property of thiolates makes the NCs positively charged, and the removal of the ligands restores the neutral valence state. Overall, our experimental results shed light on the catalytic mechanism by using atomically precise gold NCs, which offers some clues for designing more efficient catalysts.

References:

[1] a. Chong H B, Li P, Xiang J, *et al.* Design of an ultrasmall Au nanocluster-CeO_2 mesoporous nanocomposite catalyst for nitrobenzene reduction[J]. *Nanoscale*, 2013, **5**(16): 7622-7628.

b. Zhu Lin-hua(祝琳华), Li Feng-long(李奉隆), Si Tian(司 甜), *et al.* Preparation of layered clay-supported gold catalysts and catalytic activity for CO oxidation at room temperature(层状粘土负载的金催化剂制备及其常温催化氧化活性)[J]. *J Mol Catal(China)*(分子催化), 2016, **30**(1): 46-53.

c. Dou Bo-xin(窦博鑫), Xin Jia-ying(辛嘉英), Fan Hong-chen(范洪臣), *et al.* Functional self-assembly gold nanoparticle modified electrodes and application in the field of biosensors with enzyme immobilization(功能化金纳米修饰电极自组装及其在 固定化酶生物传感器中应用)[J]. *J Mol Catal(China)*(分子催化), 2016, **30**(4): 391-400.

d. Luo Fa-guo(罗发国), Li Jun(李 俊), Li Heng-feng(李衡峰). Green Synthesis of Carboxylic Acid Using Poly(Amic Acid) Salt-Stabilized Gold Nanoparticles(聚酰胺酸盐稳定的金纳米催化剂用于羧酸的绿色合成)[J]. *J Mol Catal(China)*(分子催化), 2017, **31**(1): 30-37.

e. Li Chun-yu(李春雨), Xin Jia-ying(辛嘉英), Lin Hui-ying(林惠颖), *et al.* Study on functionalized gold nanoparticles of methanobactin by copper ion coordination uesd as simulated peroxidase(铜离子配位甲烷氧化菌素功能化纳米金模拟过氧化物酶的研究)[J]. *J Mol Catal(China)*(分子催化), 2017, **31**(5): 480-485.

f. Dou Bo-xin(窦博鑫), Xin Jia-ying(辛嘉英), Wang Zhen-xing(王振兴), *et al.* Multilayer self-assembly modified electrode of methanobactin functionalized gold nanoparticle to catalytic reduction of hydrogen peroxide (甲烷氧化菌素功能化金纳米层层自组装修饰电极上过氧化氢的催化还原)[J]. *J Mol Catal(China)*(分子催化), 2017, **31**(6): 534-543.

[2] Kukushkin V Y, Pombeiro A J L. Additions to metal-activated organonitriles[J]. *Chem Rev*, 2002, **102**(5): 1771-1802.

[3] Li G, Jin R C. Catalysis by gold nanoparticles: carbon-carbon coupling reactions[J]. *Nanotechnol Rev*, 2013, **2**(5): 529-545.

[4] Zhu Y, Qian H F, Jin R C. An Atomic-level strategy for unraveling gold nanocatalysis from the perspective of $Au_n(SR)_m$ nanoclusters[J]. *Chem Eur J*, 2010, **16**(37): 11455-11462.

[5] Zhu Y, Wu Z K, Gayathri C, *et al*. Exploring stereoselectivity of Au_{25} nanoparticle catalyst for hydrogenation of cyclic ketone[J]. *J Catal*, 2010, **271**(2): 155-160.

[6] Zhu Y, Qian H F, Jin R C. Catalysis opportunities of atomically precise gold nanoclusters[J]. *J Mater Chem*, 2011, **21**(19): 6793-6799.

[7] Liu Y M, Tsunoyama H, Akita T, *et al.* Aerobic oxidation of cyclohexane catalyzed by size-controlled au clusters on hydroxyapatite: Size effect in the sub-2 nm regime [J]. *ACS Catal*, 2010, **1**(1): 2-6.

[8] Li G, Jiang D E, Kumar S, *et al.* Size dependence of atomically precise gold nanoclusters in chemoselective hydrogenation and active site structure[J]. *ACS Catal*, 2014, **4**(8): 2463-2469.

[9] Su Lin-lin(苏琳琳), Zuo Chuan(左川), Hou Wenming(候文明) *et al.* Dimensional effect of nano-Au/C catalysts in reaction of glyoxal to glyoxalic acid (纳米 Au/C 催化剂在乙二醛转化为乙醛酸反应中的尺寸效应)[J]. *Nonf Met Engineer*(有色金属工程), 2016, **2**(6): 6-10.

[10] Li G, Jin R C. Atomically precise gold nanoclusters as new model catalysts[J]. *Acc Chem Res*, 2013, **46**(8): 1749-1758.

[11] Li G, Qian H F, Jin R C. Gold nanocluster-catalyzed selective oxidation of sulfide to sulfoxide[J]. *Nanoscale*, 2012, **4**(21): 6714-6717.

[12] Li G, Jiang, D E, Liu C, *et al.* Oxide-supported atomically precise gold nanocluster for catalyzing Sonogashira cross-coupling[J]. *J Catal*, 2013, **306**(0): 177-183.

[13] Li G, Zeng C J, Jin R C. Thermally robust $Au_{99}(SPh)_{42}$ nanoclusters for chemoselective hydrogenation of nitrobenzaldehyde derivatives in water[J]. *J Am Chem Soc*, 2014, **136**(9): 3673-3679.

[14] Li G, Liu C, Lei Y, *et al.* Au_{25} nanocluster-catalyzed ullmann-type homocoupling reaction of aryl iodides [J]. *Chem Commun*, 2012, **48**(98): 12005-12007.

[15] Liu Y M, Tsunoyama H, Akita T, *et al.* Efficient and selective epoxidation of styrene with TBHP catalyzed by Au_{25} clusters on hydroxyapatite[J]. *Chem Commun*, 2010, **46**(4): 550-552.

[16] Chai J S, Chong H B, Wang S X, et al. Controlling the selectivity of catalytic oxidation of styrene over nanocluster catalysts [J]. *RSC Adv*, 2016, **6**(112): 111399-111405.

[17] Xie S H, Tsunoyama H, Kurashige W, *et al.* Enhancement in aerobic alcohol oxidation catalysis of Au25 clusters by single Pd atom doping[J]. *ACS Catal*, 2012, **2**(7): 1519-1523.

[18] Fujitani T, Nakamura I. Mechanism and active sites of the oxidation of CO over Au/TiO_2[J]. *Angew Chem Inter Edit*, 2011, **50**(43): 10144-10147.

[19] Zhu Y, Qian H, Zhu M, *et al.* Thiolate-protected Au nanoclusters as catalysts for selective oxidation and hydrogenation processes[J]. *Adv Mater*, 2010, **22**(17): 1915-1920.

[20] Zhu Y, Qian H, Drake B A, *et al.* Atomically precise $Au_{25}(SR)_{18}$ nanoparticles as catalysts for the selective hydrogenation of α,β-unsaturated ketones and aldehydes [J]. *Angew Chem Inter Edit*, 2010, **49**(7): 1295-1298.

[21] Han P, Axnanda S, Lyubinetsky I, *et al.* Atomic-scale assembly of a heterogeneous catalytic Site[J]. *J Am Chem Soc*, 2007, **129**(46): 14355-14361.

[22] Kauffman D R, Alfonso D, Matranga C, *et al.* Experimental and computational Investigation of Au_{25} clusters and CO_2: A unique interaction and enhanced electrocatalytic activity[J]. *J Am Chem Soc*, 2012, **134**(24): 10237-10243.

[23] Kauffman D R, Alfonso D, Matranga C, *et al.* Probing active site chemistry with differently charged Au_{25}^{q} nanoclusters (q = -1, 0, +1) [J]. *Chem Sci*, 2014, **5**(8): 3151-3157.

[24] Liu Ming-hua(刘鸣华). Ligand effects in catalysis by atomically precise gold nanoclusters (原子精确的金纳米团簇在催化中的配体效应)[J]. *Acta Phys -Chim Sin*(物理化学学报), 2018, **34**(6): 553-554.

[25] He L, Lou X B, Ni J, *et al.* Efficient and clean gold-cat-

alyzed one-pot selective N-Alkylation of amines with alcohols [J]. *Chem Eur J*, 2010, **16**(47): 13965-13969.

[26] Campisi S, Schiavoni M, Chan-Thaw C, *et al.* Untangling the role of the capping agent in nanocatalysis: Recent advances and perspectives[J]. *Catalysts*, 2016, **6**(12): 185-206.

[27] Zhang B, Fang J, Li J G, *et al.* Soft, Oxidative stripping of alkyl thiolate ligands from hydroxyapatite-supported gold nanoclusters for oxidation reactions[J]. *Chem Asian J*, 2016, **11**(4): 532-539.

[28] Sun H, Su F Z, Ni J, *et al.* Gold supported on hydroxyapatite as a versatile multifunctional catalyst for the direct tandem synthesis of imines and oximes[J]. *Angew Chem Inter Edit*, 2009, **48**(24): 4390-4393.

[29] Feng L, Chong H B, Li P, *et al.* Pd-Ni alloy nanoparticles as effective catalysts for miyaura-heck coupling reactions[J]. *J Phys Chem C*, 2015, **119**(21): 11511-11515.

[30] Garigipati R S. An efficient conversion of nitriles to amidines [J]. *Tetra Lett*, 1990, **31**(14): 1969-1972.

[31] Zhong R Y, Sun K Q, Hong Y C, *et al.* Impacts of organic stabilizers on catalysis of Au nanoparticles from colloidal preparation[J]. *ACS Catal*, 2014, **4**(11): 3982-3993.

[32] Bailie J E, Hutchings G J. Promotion by sulfur of gold catalysts for crotyl alcohol formation from crotonaldehyde hydrogenation[J]. *Chem Commun*, 1999, **21**: 2151-2152.

[33] Corbin W C, Nichol G S, Zheng Z. Amidine production by the addition of NH_3 to nitrile(s) bound to and activated by the lewis acidic $[Re_6(\mu_3\text{-}Se)_8]^{2+}$ cluster core [J]. *Inorg Chem*, 2016, **55**(19): 9505-9508.

[34] Li G, Abroshan H, Liu C, *et al.* Tailoring the electronic and catalytic properties of Au_{25} nanoclusters via ligand engineering [J]. *ACS Nano*, 2016, **10**(8): 7998-8005.

[35] Li J, Nasaruddin R R, Feng Y, *et al.* Tuning the accessibility and activity of $Au_{25}(SR)_{18}$ nanocluster catalysts through ligand engineering[J]. *Chem Eur J*, 2016, **22**(42): 14816-14820.

[36] Jin R C, Zeng C J, Zhou M, *et al.* Atomically precise colloidal metal nanoclusters and nanoparticles: fundamentals and opportunities[J]. *Chem Rever*, 2016, **116**(18): 10346-10413.

[37] Chen S, Xiong L, Wang S X, *et al.* Total structure determination of $Au_{21}(S\text{-}Adm)_{15}$ and geometrical/electronic structure evolution of thiolated gold nanoclusters[J]. *J Am Chem Soc*, 2016, **138**(34): 10754-10757.

[38] Zhu M Z, Qian H F, Jin R C. Thiolate-protected $Au_{24}(SC_2H_4Ph)_{20}$ nanoclusters: superatoms or not[J]. *J Phys Chem Lett*, 2010, **1**(6): 1003-1007.

[39] Zhu M Z, Qian H F, Jin R C. Thiolate-protected Au_{20} clusters with a large energy gap of 2.1 eV[J]. *J Am Chem Soc*, 2009, **131**(21): 7220-7221.

[40] Zhu M Z, Lanni E, Garg N, *et al.* Kinetically controlled, high-yield synthesis of Au_{25} clusters[J]. *J Am Chem Soc*, 2008, **130**(4): 1138-1139.

[41] Zheng J, Wu B H, Jiang Z Y, *et al.* General and facile syntheses of metal silicate porous hollow nanostructures [J]. *Chem Asian J*, 2010, **5**(6): 1439-1444.

选择性控制的配体工程在金团簇催化中的作用

高贵琪[2], 崇汉宝[1,2], 李 广[1*]

(1. 安徽大学 物理工程学院,安徽 合肥 230601;
2. 安徽大学 物质科学与信息技术研究院,安徽 合肥 230601)

摘要: 金团簇表面的硫醇配体影响着团簇的催化性质, 尤其是选择性. 我们采用在真空条件下通过程序升温的方法逐渐剥除金团簇表面的硫醇配体来制备催化剂, 利用透射电镜, 红外光谱对催化剂结构进行表征, 以硝基化合物催化还原反应为模型反应, 详细研究了配体对催化活性和选择性的影响. 研究发现因配体被剥离导致底物更容易接近团簇表面, 最终使得反应转换率大幅升高. 实验结果还表明金团簇催化剂催化不同官能团取代的底物显示了良好的官能团兼容性, 有吸电子效应的硫配体使团簇表面带正电荷, 进而避免苯胺衍生物的产生.

关键词: 配体效应; 选择性; 金团簇; 催化; 纳米